

Temperature Profile Estimation in the Core of a Sodium-Cooled Fast Reactor using CFD Modeling

Estimación del Perfil de Temperaturas en el Núcleo de un Reactor Rápido Refrigerado por sodio mediante modelado CFD

DIAZ-ESPINOZA, Gerardo*†, VALLE-HERNANDEZ, Julio and GALLARDO-VILLARREAL, José Manuel

*Universidad Politécnica Metropolitana de Hidalgo
Universidad Autónoma del Estado de Hidalgo*

ID 1st Author: *Gerardo, Diaz Espinoza* / ORC ID: 0000-0003-1293-0275, CVU CONACYT ID: 926199

ID 1st Co-author: *Julio, Valle-Hernandez* / ORC ID: 0000-0001-8957-0066, CVU CONACYT ID: 210743

ID 2nd Co-author: *José Manuel, Gallardo Villarreal* / ORC ID: 0000-0002-7578-7229, CVU CONACYT ID: 366394

DOI: 10.35429/JSL.2022.26.9.31.39

Received March 30 2022; Accepted June 30, 2022

Abstract

The latest proposal for nuclear systems for application in space are 4th generation reactors that use liquid metals as coolant. The operating conditions, as well as its safety in these matters, is linked to its thermal and fluid dynamic behavior. This paper presents the estimation of the temperature profile of a sodium-cooled fast reactor from the conduction and convection heat transfer mechanisms. The temperature distribution is analyzed in the area of the fuel and the temperature profile of the coolant in the area of the high conductivity pipes. Is established the analysis of nuclear fuel in a one-dimensional, stationary and with power generation. In the GAP area, the analysis is carried out by natural convection, and finally, the cladding in contact with sodium by forced conduction-convection. As results, it is presented the simulation in Computational Fluid Dynamics to determine the temperature profile due to the behavior of the coolant in the pipe when subjected to a constant flow of heat supplied by the nuclear fuel pellets. The temperature profile will allow us to determine the parameters to establish the operating conditions of secondary power conversion systems.

Resumen

La última propuesta de sistemas nucleares para su aplicación en el espacio son los reactores de 4ta generación que utilizan metales líquidos como refrigerante. Las condiciones de operación, así como su seguridad en estos temas está ligado a su comportamiento térmico y fluidodinámico. En este trabajo se presenta la estimación de perfil de temperaturas de un reactor rápido refrigerado por sodio a partir de los mecanismos de transferencia de calor por conducción y convección. La distribución de temperaturas se analiza en la zona del combustible y el perfil de temperatura del refrigerante en la zona de las tuberías de alta conductividad. El análisis del combustible nuclear se establece de manera unidimensional, estacionaria y con generación de energía. En la zona del GAP el análisis se realiza mediante convección natural, finalmente la zona del revestimiento en contacto con el sodio por conducción-convección forzada. Como resultados se presenta la simulación en Dinámica de Fluidos Computacional para determinar el perfil de temperatura debido al comportamiento del refrigerante en la tubería al ser sometida a un flujo constante de calor suministrado por las pastillas de combustible nuclear. El perfil de temperatura nos permitirá determinar los parámetros para establecer las condiciones de operación sistemas secundarios de conversión de potencia.

Fluids, Flow, Nuclear Reactor, Heat, Transfer, Analysis

Fluidos, Flujo, Reactor Nuclear, Heat, Transfer, Analysis

Citation: DIAZ-ESPINOZA, Gerardo, VALLE-HERNANDEZ, Julio and GALLARDO-VILLARREAL, José Manuel. Temperature Profile Estimation in the Core of a Sodium-Cooled Fast Reactor using CFD Modeling. Journal Simulation and Laboratory. 2022, 9-26: 31-39

*Correspondence to Author (e-mail: 213220016@upmh.edu.mx)

†Researcher contributing as first Author.

1. Introduction

The development of new categories of nuclear reactors involves the use of liquid metals as coolant. Unlike thermal reactors that use water as coolant and moderator, fast reactors cooled by liquid metals do not use a moderator (12), because the neutrons generated in the fission process have high energy and move quickly, providing a more efficient system with characteristics to withstand high operating temperatures.

The heating and cooling of fluids inside high conductivity pipes are recurrent heat transfer processes in nuclear systems, being the heating of the coolant by extracting heat from the fuel pellets and the cooling of the coolant by circulating throughout the system, this process allows transferring heat to another area of the system where it is required; the latter establishes the parameterization of subsequent components either heat exchangers or power converters.

This configuration allows to define the nuclear system that we will analyze in this article, being the Lunar Evolutionary Growth Optimized (LEGO) Nuclear Reactor the one implemented to supply electric power for possible lunar settlements. As characteristics it presents Uranium Dioxide (UO₂) as nuclear fuel stored in 84 pellets, contained in a helium gap and SS-316 stainless steel cladding, 43 high conductivity pipes and cooled by sodium, delivering a thermal power of 24 kWt.

Therefore, observing the behavior of the coolant in this type of nuclear reactors will be the main objective of this article, the characteristics of the transport of liquid metal as coolant through the high conductivity pipes of the reactor system will be taken into consideration and a heat transfer analysis will be performed by CFD modeling that will allow obtaining temperature profiles in certain cross sections of the pipe, giving guideline to observe the final temperature at the outlet of the same.

2. Methodology

The methodology developed in this work is presented below:

- Description of the Lunar Nuclear Reactor
- Mathematical foundation for system analysis.

- Heat Transfer Model
- Initial Coolant Parameters at the Inlet of High Conductivity Pipelines.
- System Modeling in Computational Fluid Dynamics
- Estimation of the temperature transferred from the nuclear reactor to the coolant.

3. Description of the Lunar Nuclear Reactor

The Lunar Evolutionary Growth Optimized (LEGO) Reactor contains stainless steel clad UO₂ fuel pellets that are structurally and thermally bonded to high conductivity pipes carrying sodium. Heat is conducted from the fuel pellets to the pipes, which then carry the heat to a power conversion system (1).

It is a type of Clustered Lunar Regolith Reactor and called Advanced Generation 4 because it is a liquid metal-cooled Fast Reactor composed of six subcritical nuclear reactor subunits capable of generating up to 24 kWt each. A fundamental group composed of six subunits provides 30 kWe to a lunar base.

3.1. Reactor Core Geometry

The LEGO reactor uses the existing lunar regolith as a radiation shielding material and neutron reflector. Each subunit is embedded in the lunar surface to create a neutron-coupled reactor assembly capable of reaching criticality to generate power. The reactor subunits have a subcritical design, which promotes safety in the event of a launch accident (1).

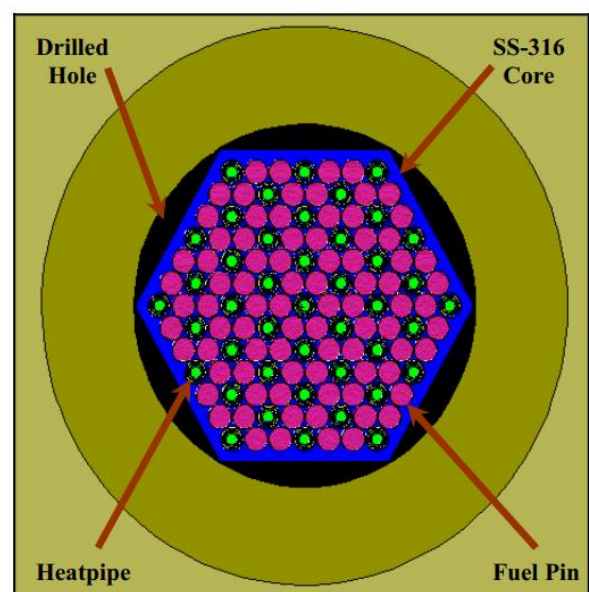


Figure 1 Top (1) and Isometric view of the core of a LEGO Reactor subunit

Fast fission reactor systems are capable of fissioning any additional actinides produced in the fuel and can achieve deeper burnup levels than conventional thermal reactors. The lower operating power per subunit reduces neutron damage and thermal loads compared with larger reactor systems, which increases the longevity of the intrinsic properties of the reactor materials (1).

3.2. Characteristics of the Fuel Assemblies

It is composed of enriched Uranium Dioxide (UO₂), and for the system lining of austenitic stainless steel (SS-316) containing molybdenum, being more resistant to corrosion offering higher creep, stress to rupture and tensile strength at elevated temperatures (16).

This hexagonal packing configuration allows a high heat transfer ratio and is designed to deliver 24 kWt to the power conversion system. The core has 84 fuel rods and 43 high-conductivity pipes that carry the metallic liquid (sodium) (1).

The fuel rods have a diameter of 1.6160 cm contained in 1.6414 cm (SS-316) tubing with helium-filled spaces. The high conductivity pipes are modeled with a 1.1254 cm SS-316 casing with a 0.7878 cm SS-316 wick and 0.0844 cm thickness (1).

The fuel is 93% enriched in ²³⁵U at 95% of theoretical density. The fuel rods are 49 cm long with a total core height of 54 cm; high conductivity tubing extends an additional 106 cm above the core. The SS-316 monolithic hexagonal core design has a circumscribed corner-to-corner diameter of 23.80 cm.

A tapered stainless steel base extends 9 cm below the core to provide support, stability and alignment within the drilled hole (1).

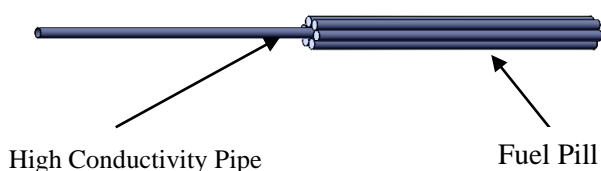


Figure 2 Side view of the core of a LEGO Reactor subunit section

Parameters	
Fuel Pad Diameter (m)	0.016414
High Conductivity Pipe Diameter (m)	0.011254
Coating Thickness (m)	0.000844
High Conductivity Pipe Length (m)	1.06
Length Fuel Pads (m)	0.49

Table 1 Geometric Parameters of the Model (1)

3.3. Coating

For the SS-316 stainless steel alloy used on the surface of high conductivity pipes, the addition of austenitic chromium-nickel with molybdenum increases corrosion resistance and improves pitting resistance to chloride ion solutions and provides higher resistance to elevated temperatures (17).

3.4. Reactor Coolant

Due to the large amount of energy released by the core, a working fluid with good heat transfer characteristics is used. The LEGO reactor, being a fast reactor, uses a liquid metal-based coolant system, being sodium the one assigned to extract the emitted heat and having as an advantage that it can remain in liquid state in a high temperature range (1).

To keep the sodium as a suitable candidate, it is established that, compared with other refrigerants used in terrestrial counterparts, sodium has a low need for pumping power, can be used at atmospheric pressure, works well below the boiling point which makes possible its ability to absorb considerable energy in emergency conditions (3).

Likewise, it is a fluid with a tendency to dissolve penetrating fission products due to some failure, as well as to retain them.

4. Mathematical Foundation for System Analysis

The simulation of the phenomena corresponding to fluid-dynamic perturbations in systems represents the response of fluids to mechanical forces, motion and heat transfer. To observe this behavior, the conservation of energy, conservation of momentum and conservation of mass equations are defined. (2).

4.1. Conservation of mass

The mass balance through the control volume is expressed by the continuity equation:

$$\frac{\partial \rho}{\partial t} + \nabla \cdot (\rho \vec{v}) = 0 \quad (1)$$

where ρ is the density of the fluid, i.e. the mass per unit volume, \vec{v} is the velocity field and t the time variable.

4.2. Conservation of Momentum

Since the external forces acting on a control volume are represented by the ratio of change with respect to time of the linear momentum and the flow over a surface is expressed by:

$$\rho \frac{\partial \vec{v}}{\partial t} + \rho (\vec{v} \cdot \nabla) \vec{v} = -\nabla p + \rho \vec{g} + \nabla \cdot \tau_{ij} \quad (2)$$

where \vec{g} the acceleration of gravity, τ_{ij} , the viscous stress tensor;

4.3 Energy Conservation

$$\rho \frac{\partial E}{\partial t} + \rho \nabla \cdot (\vec{v} E) = \nabla \cdot (k \nabla T) + \rho \vec{g} \cdot \nabla (\sigma \cdot \vec{v}) + W_f + \dot{q}_H \quad (3)$$

where E is the fluid energy, T the temperature, k the thermal conductivity, \vec{g} the acceleration of gravity, σ the stress tensor; W_f the work done on the fluid and (\dot{q}_H) the heat supplied to the fluid.

However, there are phenomena that introduce additional nonlinearities, such as turbulence or chemical reactions.

This makes it impossible to obtain an analytical solution, making it necessary to resort to approximate methods, such as numerical techniques, for its solution. (18).

5. Heat Transfer Model

5.1. Heat Transfer in the Fuel Cell

It is important to know the temperature distribution in the system, so it is considered to perform the analysis in cylindrical coordinates as follows:

$$\frac{1}{r} \frac{\partial}{\partial r} \left(kr \frac{\partial T}{\partial r} \right) + \frac{1}{r^2} \frac{\partial}{\partial \phi} \left(kr \frac{\partial T}{\partial r} \right) + \frac{\partial}{\partial z} \left(k \frac{\partial T}{\partial r} \right) + e_{gen} = \rho c \frac{\partial T}{\partial t} \quad (4)$$

For this article, the centerline is taken as the origin of the r -coordinate. Due to the symmetry in the z -direction and the azimuthal direction, we can separate the variables and simplify the problem in a one-dimensional way, as well as:

1. Heat conduction in the axial direction is negligible with respect to heat conduction in the radial direction.
2. Heat generation in the fuel is uniform at each of the radial nodes.
3. The heat transfer is considered stationary for the system.
4. No heat generation in the coating.

Thus the above equation simplifies to:

$$\frac{1}{r} \frac{\partial}{\partial r} \left(kr \frac{\partial T}{\partial r} \right) + \frac{q_v}{k} = 0 \quad (5)$$

5.2. Heat Transfer at the GAP

Natural Convection

For a system of concentric cylinders the natural convection heat transfer rate is expressed as:

$$\dot{Q} = \frac{2\pi k_{eff}}{\ln\left(\frac{D_o}{D_i}\right)} (T_i - T_o) \quad (6)$$

where k_{eff} is the effective thermal conductivity, i.e., for convective heat transfer in a closed room it is analogous to conduction whenever it is replaced as $k_{eff} = kNu$.

For the analysis of the Nusselt number in natural convection, the heat transfer relationships based on experimental studies are taken, which determines that:

$$Nu = \frac{hLc}{k} = C(Gr_L Pr) = C Ra_L \quad (7)$$

Where $[Ra]_L$ is the Rayleigh number, which is the product of the Grashof and Prandtl numbers; which describes the relationship between buoyancy and viscosity within the fluid, and the Prandtl number, which describes the relationship between the diffusivity of the quantity of motion and the thermal diffusivity; therefore, it will be obtained that

$$Ra_L = Gr_L Pr = \frac{g\beta(T_s - T_\infty)Lc^3}{\nu^2} Pr = \frac{g\beta(T_s - T_\infty)Lc^3}{\nu\alpha} \quad (8)$$

Being g the gravity, β the coefficient of volumetric expansion, T_s the surface temperature, T_∞ the temperature of the fluid far enough from the surface, Lc the characteristic length of the geometric configuration and ν the kinematic viscosity of the fluid.

For steady flow heat at the surface, the ratio is known to be $Q = q_s A_s$, not knowing the surface temperature, it is related to the uniform flow characteristics which allows relating the Rayleigh interval to the Nusselt number for certain geometric configuration, as shown in the following equation.:

$$Nu = \left\{ 0.825 + \frac{0.387 Ra_L^{\frac{1}{4}}}{\left[1 + \left(\frac{0.492}{Pr} \right)^{\frac{9}{16}} \right]^{\frac{8}{27}}} \right\}^2 \quad (9)$$

The correlation of heat transfer by natural convection in the subchannel in the developing region for a constant heat flux can be formulated as follows:

$$Nu = C(Gr_L Pr) \quad (10)$$

5.3. Heat Transfer in Coatings

– Coolant

Forced Internal Convection

This last section of the heat transfer mechanisms presents the forced convection as part of the mathematical model to be verified by numerical simulation, this because the coolant was forced through the pipes this mechanism establishes the extraction of heat from the reactor, so it is defined as follows:

If the heat transfer coefficient is known for a given geometry and specific flow conditions, the rate of heat transfer at the prevailing temperature difference can be calculated using Equation 11

$$q_c = h_c A (T_s - T_\infty) \quad (11)$$

Where q_c is the heat flux, h_c is the convective heat transfer coefficient, T_s is the surface temperature and T_∞ is the fluid temperature. For the analysis of heat transfer by forced convection, the following correlation is presented, which allows observing the behavior of the fluid flow involving the thermal conductivity, the specific heat and the type of flow it has:

$$Nu = (Re Pr) \quad (12)$$

Where:

$$Nu = \text{Número de Nusselt} = \frac{hD}{k}$$

$$Re = \text{Número de Reynolds} = \frac{\rho V D}{\mu}$$

$$Pr = \text{Número de Prandtl} = \frac{c_p \mu}{k}$$

Likewise, the Dittus-Boelter correlation is implemented for heated fluid and turbulent flow to calculate the Nusselt flow number in a circular pipe based on equation 12.

$$Nu = 0.023 Re^{0.8} Pr^{0.4} \quad (13)$$

Finally, by relating equations 12 and 14, the value of the convective heat transfer coefficient is determined, obtaining:

$$h = \frac{Nu k}{Dh} \quad (14)$$

where Dh is the hydraulic diameter where it involves the Area and Perimeter of the pipeline.

6. Initial Parameters for Numerical Modeling

The properties of the coolant are represented due to its behavior in certain temperature ranges, for this article the interpolation polynomials were generated referring to that variation that may exist throughout the flow section.

Following are the properties that were determined by the interpolation function:

Thermal Conductivity $\left(\frac{W}{mK} \right)$

$$k = 91.8 - (49 * 10^{-3})T + (3.469 * 10^{-18})T^2 - (3.881 * 10^{-21})T^3 + (1.6544 * 10^{-24})T^4 \quad (15)$$

Specific Heat $\left(\frac{J}{kg \cdot ^\circ C}\right)$

$$Cp = 1435.9 - (0.5700643)T + (0.0004275833)T^2 + (0.0000000439286)T^3 - (19.04 * 10^{-12})T^4 \quad (16)$$

Dynamic Viscosity $\left(\frac{Pa}{s}\right)$

$$\mu = 0.0011017 - 0.0000054859T + (1.43913 * 10^{-8})T^2 - (1.76067 * 10^{-11})T^3 + (87.8667 * 10^{-15})T^4 \quad (17)$$

Density $\left(\frac{kg}{m^3}\right)$

$$\rho = 949.93 - (226.6 * 10^{-3})T - (2.61667 * 10^{-5})T^2 + (2.25 * 10^{-8})T^3 - (8.3333 * 10^{-12})T^4 \quad (18)$$

The LEGO reactor is designed for a high thermal power range, so the thermal behavior of the walls of the system is bounded by the characteristics of the coating material, for the case of the walls of the pipes high conductivity temperature limit is 1250 K (977 °C).

For the coating implemented in the pipes, we will assign the values that are thermal conductivity, specific heat and density for stainless steel that will provide an approximation of the behavior of the wall with the flow of the coolant to provide a constant flow of heat.

Parameters	
Thermal Conductivity $\left(\frac{W}{mK}\right)$	16.2
Specific Heat $\left(\frac{J}{kgK}\right)$	502.48
Density $\left(\frac{kg}{m^3}\right)$	8030

Table 2 Coating Parameters

The following considerations will be taken into account to carry out the CFD modeling, initially it is taken as an internal flow, because it will be confined in a pipe, it is established to work with a turbulent flow.

An analysis of forced internal convection will be handled since the coolant will be forced to flow through the high conductivity pipe involving stationary conditions, i.e., the fluid properties will not change with respect to time, only with respect to temperature.

Finally, it will take into account a one-dimensional analysis, the fluid properties will vary in one direction only.

Parameters	
Speed $\left(\frac{m}{s}\right)$	5.02
Fluid inlet temperature (°C)	800
Heat Flow $\left(\frac{MW}{m^2}\right)$	1.64

Table 3 Wall Parameters

To obtain the temperature profiles, the position of the coolant flow is presented as longitudinal through the high conductivity pipe, the temperature values were obtained due to the constant flow of heat in the wall of the entire section.

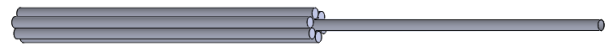


Figure 3 Side View of Coolant Flow in Position to CFD Modeling

7. Results

7.1. Temperature Distribution - Fuel

Next, the results obtained from the analytical calculation obtained due to the heat transfer mechanisms by conduction Eq. (5) and convection Eq. (11) in the fuel zone, the GAP and the cladding as a function of the thermal power of the fuel and the coolant flow are presented.

In Figure 4, the heat transfer by conduction is implemented in a one-dimensional and stationary way, due to these considerations the heat transfer equation by conduction in cylindrical coordinates is simplified, allowing to observe the behavior of the temperature in a radial way.

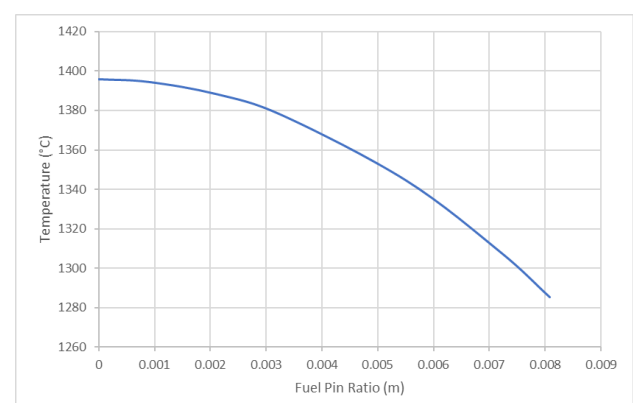


Figure 4 Temperature Distribution - Fuel Cylinder

Using the boundary conditions at $T(0)$ and $T(r)$, the equation was obtained to determine the temperature at each radial node generating the temperature distribution up to the outer wall of the fuel pellet GAP is found.

7.2. Temperature Distribution - GAP

The fission gases are released to the free volume of the rod, which increases the internal pressure causing the nuclear fuel to swell, this zone is filled with helium so the heat transfer in this section will be analyzed by natural convection, it has been taken into account a series of dimensionless numbers that allow observing the behavior when subjected to the thermal power of the fuel.

The parameterization of this zone was carried out by means of the Nusselt number, which correlates to the Rayleigh number and the Prandtl number Eq. (7). Taking into account the gravity of the moon simulating a mission in that site, the value will be taken as $g=1.62 \text{ m/s}^2$, likewise the kinematic viscosity of helium being $\nu=0.000158359 \text{ m}^2/\text{s}$, based on Eq. (8) we can obtain the Grashof number. Subsequently, the Prandtl number relating the dynamic viscosity and thermal conductivity can be correlated with the Grashof number to determine the Rayleigh number.

Being the Rayleigh number a guideline to determine the Nusselt number which, establishing the variation of the same in each value of the radius in the thickness of the GAP, the temperature distribution is determined as shown in the following figure.

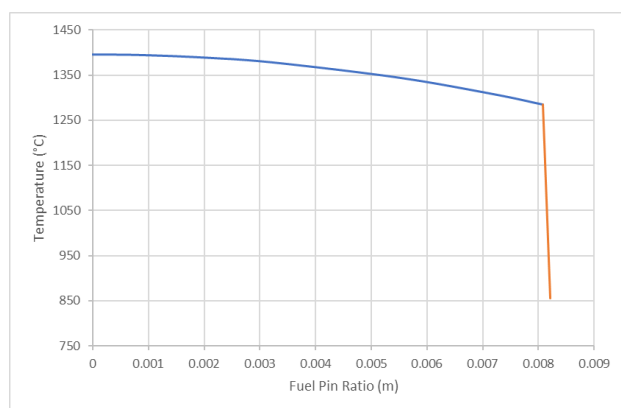


Figure 5 Fuel Temperature Distribution – GAP

Finally, the properties of sodium are presented by means of the interpolation polynomials (Equation 15-18) that are affected by the temperature changes to which it will be subjected. The value of the mass flow is proposed which, based on the area of the pipe and the density of the fluid, the velocity at which it will flow in that cross section can be obtained, thus obtaining $v = 6.85 \frac{\text{m}}{\text{s}}$

Having the speed and properties of the coolant at an average temperature, we proceed to apply Eq. (12) to determine the Prandtl and Reynolds number, the Dittus - Boelter correlation marks the starting point to implement the above dimensionless numbers, obtaining the value of the Nusselt number of 46.12. By means of equation 14, the convective heat transfer coefficient is obtained being $h=202 \text{ kW}/(\text{m}^2 \text{ C})$ which allowed based on equation 11 to obtain the wall temperature due to the temperature at the proposed outlet, this temperature assumption, was obtained by varying values to achieve the thermal power of the reactor.

By the above variation, the temperature of the wall that will be in contact with the coolant was obtained, which will not allow to obtain the heat loss due to the internal wall temperature of the liner and the new temperature taking into account that a $\Delta T=429 \text{ }^\circ\text{C}$ was determined. Based on this value, the heat loss in the entire liner section was determined.

7.3. Temperature Distribution - Coating

Finally, implementing the conduction heat conduction equation in cylindrical coordinates, the temperature distribution is determined by knowing the heat loss in the coating, obtaining Figure 6 according to the changes related to the GAP and its temperature distribution.

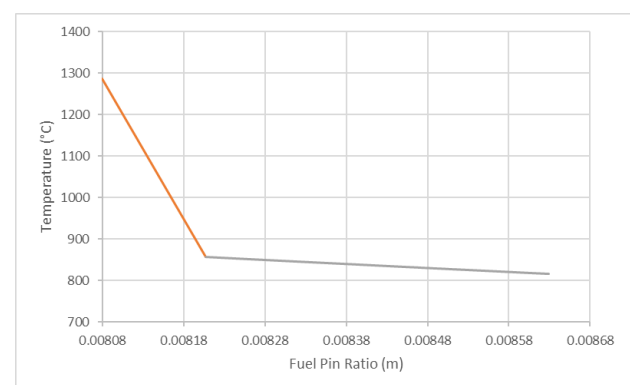


Figure 6 GAP Temperature Distribution – Coating

The ΔT s for each section and the final temperatures at each boundary are presented below.

ΔT_{Fuel}	110 °C
ΔT_{GAP}	429 °C
ΔT_{Clad}	43 °C
$T_{in} - T_{Fuel}$	1396 °C
$T_{Text} - T_{Fuel}$	1285 °C
$T_{Text} - T_{GAP}$	856 °C
$T_{Text} - T_{Revestimiento}$	812 °C

The initial parameters of the CFD modeling will be some of the values obtained analytically being the constant heat flux, the coolant inlet temperature and velocity. As a means of verification, the use of CFD techniques was implemented where the geometry of the high conductivity pipe was generated taking the diameter and length.

Likewise, the boundary conditions and the parameterization of the inlet, outlet and walls were generated obtaining the temperature profile and contour.

7.4. Temperature Profiles - Pumping Pipelines

Figure 7 shows the streamlines of the temperature change in the fluid due to a constant heat flow in the wall area, this value was obtained due to the thermal power of the fuel pellet.

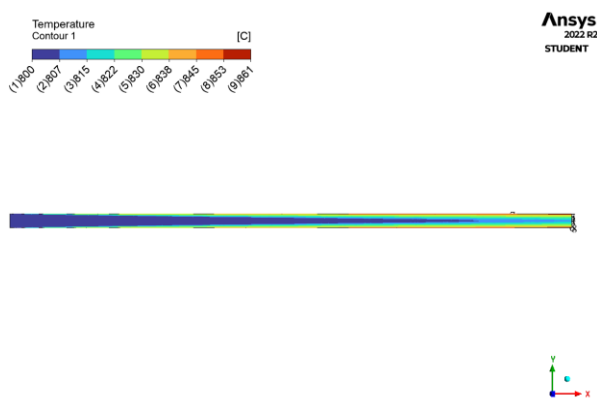


Figure 7 Power Lines – Pipelines

You can observe the temperature increase as the position of the coolant changes through the longitudinal section, in the same way the temperature at the inlet and outlet of the system will be taken as a reference, observing the temperature distribution in the coolant flow.

It could also observe the behavior of the thermal boundary layer along the entire section, mainly analyzes the thermal input region where it begins to increase the fluid temperature, to reach a point where the temperature will remain constant so it reaches the region fully developed thermally being this the area of interest for this article due to the temperature at the outlet of the pipe.

Finally, in Figure 8 you can see the temperature profile of the coolant flow to be subjected to a constant flow of heat observing the temperature distribution from the inlet temperature to the outlet temperature, this because it was determined the temperature at the wall.

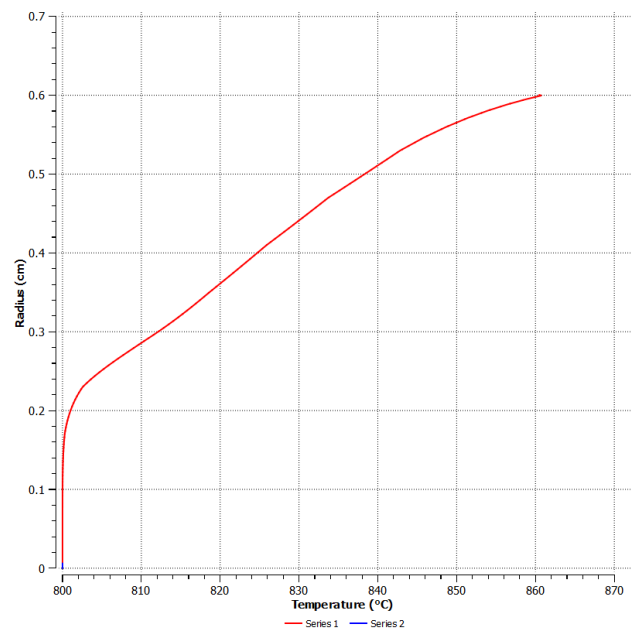


Figure 8 Coolant Flow Temperature Profiles as a function of radius

	Analytical	CFD
$T_{int} - T_{Revestimiento}$	856 °C	861 °C
$T_{Text} - T_{Revestimiento}$	815 °C	825 °C
$T_{out} - T_{Refrigerante}$	814 °C	819 °C

8. Conclusions

Based on the results obtained, the following conclusions will be presented:

- Increased heat transport due to forced coolant flow will cause a decrease in reactor temperature.
- The behavior of the temperature distribution in the reactor-coolant zone having appropriate ΔT with respect to the thermal power delivered by the nuclear reactor was observed.

- The results obtained due to the temperature distribution in the reactor area and the coolant flow will keep the coolant in liquid state, causing a redesign of the LEGO Reactor, giving guidelines for future work regarding the implementation of a pumping system that drives the coolant to the potassium boiler.
- It was observed that the temperature at the output in the CFD modeling approached with a difference of 0.8% to the analytical modeling performed.

9. Funding

This work has been funded by CONACYT Grant Number 926199.

References

- [1] Bess, John Darrell. (2008) A Basic LEGO Reactor Design for the Provision of Lunar Surface Power. United States. (INL/CON--08-14353).
- [2] Cengel, Yunus A. (2004) Transferencia De Calor Y Masa. Fundamentos y aplicaciones. University of Nevada, Reno.
- [3] Jeltsov, Marti. (2018) Validation and Application of CFD to Safety-Related Phenomena in Lead-Cooled Fast Reactors. KTH Royal Institute of Technology. Pag 15-18.
- [4] Toapanta, Ramos. Luis F. (2019) Estudio Numerico y Comparativo del Efecto de Turbulencia en Codos y Dobleces para Distribución de Agua Sanitaria. Pag 8-11.
- [5] Crevillén, García. David (2012) Simulación Numérica del Flujo a través del Tubo Difusor de una Turbina de Reacción. Factores de Mejora de su Eficiencia. Universidad Politécnica de Cartagena.
- [6] Scarpin, Gustavo (2012) Modelo Adiabático Ideal de Motores Stirling. Proyecto, Instituto Universitario Aeronáutico. DMA-003/12.
- [7] Koshkin N. I., Shirkévich M. G.. Manual de Física elemental, Edt. Mir (1975) págs. 74-75.
- [8] Park, Ye Young (2019) Design Study of Heat Pipes for Nuclear Spaceship Applications. Department of Nuclear Engineering, Ulsan National Institute of Science and Technology (UNIST), 50 UNIST-gil, Ulju-gun, Ulsan, 44919, Republic of Korea.
- [9] Sleicher, C.A., & Rouse, M.W. (1975). A convenient correlation for heat transfer to constant and variable property fluids in turbulent pipe flow. International Journal of Heat and Mass Transfer, 18, 677-683.
- [10] Palos Mario, *et al* (2019) Lunar ISRU Energy Storage And Electricity Generation, European Space Agency.
- [11] L. Mason, D. Poston, and L. Qualls. System Concepts for Affordable Fission Surface Power. Space Technology and Applications International Forum (STAIF), 2008.
- [12] INTERNATIONAL ATOMIC ENERGY AGENCY, Status of Fast Reactor Research and Technology Development, IAEA-TECDOC-1691, IAEA, Vienna (2013)
- [13] KAZACHKOVSKIY, O D *et al* , "The present status of the fast reactor programme in the USSR" (Proc. Int Conf on Nuclear Power and its Fuel Cycle, Salzburg, 1977) 1, Paper IAEA-CN-36/356, IAEA, Vienna (1977) 393-414
- [14] Khodarev, Eduard (1978) Liquid Metal Fast Breeder Reactors. International Atomic Energy Agency, Bulletin 20 (6), 29.38
- [15] Judd, W.C. *et al* (1964) Analysis Of Essential Nuclear Reactor Materials. New Brunswick Lab., AEC, NJ (United States)
- [16] Lister, Derek H. (2014) Nuclear Plant Materials and Corrosion. University of New Brunswick.
- [17] Combined Metals of Chicago (2017) Alloy 316L Stainless Steel. Bellwood Service Center. IL. USA.
- [18] Vicente, S. Pablo (2016) Análisis Termohidráulico de la Refrigeración del Combustible Nuclear mediante Dinámica de Fluidos Computacional. Universidad Politécnica de Madrid. Master en Ingeniería Industrial.